



Three-dimensional bone morphology is a risk factor for medial postmeniscectomy syndrome: A retrospective cohort study

Jonas Grammens^{1,2}   | Annemieke Van Haver^{1,3} | Femke Danckaers²  |
 Kristien Vuylsteke³  | Jan Sijbers²   | Lotem Mahluf⁴ |
 Peter Angele^{5,6}  | Elizaveta Kon^{7,8}  | Peter Verdonk^{1,9,10}   | MEFISTO WP1
 Group

¹Antwerp Surgical Training, Anatomy and Research Centre, University of Antwerp, Wilrijk, Belgium

²imec-VisionLab, Department of Physics, University of Antwerp, Wilrijk, Belgium

³More Institute, Deurne, Belgium

⁴Active Implants BV, Haarlem, Netherlands

⁵Clinic for Trauma and Reconstructive Surgery, University Hospital Regensburg, Regensburg, Germany

⁶Sportopaedicum Regensburg, Regensburg, Germany

⁷Humanitas Clinical and Research Center - IRCCS, Rozzano, Milan, Italy

⁸Department of Biomedical Sciences, Humanitas University, Pieve Emanuele, Milan, Italy

⁹Department of Orthopaedics, University Hospitals Antwerp, Edegem, Belgium

¹⁰OrthoCA, Antwerp, Belgium

Correspondence

Jonas Grammens

Email: jonas.grammens@uantwerpen.be

Funding information

European Union's Horizon 2020 research and innovation programme, Grant/Award Number: No 814444 (MEFISTO)

Abstract

Purpose: The study aims to identify differences in tibiofemoral joint morphology between responders (R group, no pain) to arthroscopic partial medial meniscectomy (APMM) versus medial postmeniscectomy syndrome patients (MPMS group, recurrent pain at 2 years postmeniscectomy) in a clinically neutrally aligned patient population. The second aim was to build a morphology-based predictive algorithm for response to treatment (RTT) in APMM.

Methods: Two patient groups were identified from a large multicentre database of meniscectomy patients at 2 years of follow-up: the R group included 120 patients with a KOOS pain score > 75, and the MPMS group included 120 patients with a KOOS pain score ≤ 75. Statistical shape models (SSMs) of distal femur, proximal tibia and tibiofemoral joint were used to compare knee morphology. Finally, a predictive model was developed to predict RTT, with the SSM-derived morphologic variables as predictors.

Results: No differences were found between the R and MPMS groups for patient age, sex, height, weight or cartilage status. Knees in the MPMS group were significantly smaller, had a wider femoral notch and a smaller medial femoral condyle. A morphology-based predictive model was able to predict MPMS at 2 years follow-up with a sensitivity of 74.9% (95% confidence interval [CI]: 74.4%–75.4%) and a specificity of 81.0% (95% CI: 80.6%–81.5%).

Conclusion: A smaller tibiofemoral joint, a wider intercondylar notch and smaller medial femoral condyle were observed shape variations related to medial postmeniscectomy syndrome. These promising results are a first

Abbreviations: 3D, three-dimensional; AP, anteroposterior; APMM, arthroscopic partial medial meniscectomy; AUC, area under the curve; BMI, body mass index; CI, confidence interval; IKDC, International Knee Documentation Committee; KOOS, Knee injury and Osteoarthritis Outcome Score; ML, mediolateral; MPMS, medial postmeniscectomy syndrome; MRI, magnetic resonance imaging; n.s., nonsignificant; OA, osteoarthritis; PACS, picture archiving and communication system; PC, principal component; PCA, principal component analysis; PD, proton density; PROM, patient-reported outcome measure; RMSE, root mean square error; ROC, receiver operating characteristic; RTT, response to treatment; R group, responder group; SD, standard deviation; SSM, statistical shape model.

This is an open access article under the terms of the [Creative Commons Attribution](https://creativecommons.org/licenses/by/4.0/) License, which permits use, distribution and reproduction in any medium, provided the original work is properly cited.

© 2024 The Author(s). *Journal of Experimental Orthopaedics* published by John Wiley & Sons Ltd on behalf of European Society of Sports Traumatology, Knee Surgery and Arthroscopy.

step towards a knee morphology-based clinical decision support tool for meniscus treatment.

Study Design: Case–control study.

Level of Evidence: Level IIIb.

KEYWORDS

3D, knee, meniscectomy, morphology, predictive model

INTRODUCTION

Among possible surgical treatment options for medial meniscal tears, arthroscopic partial medial meniscectomy (APMM) is one of the most regularly performed knee surgery worldwide [7, 18, 24, 25, 46]. Recent insights have resulted in an evolution of its indications [38], and there is a paradigm shift towards preserving the meniscus to the greatest extent possible [1].

Current guidelines [6, 26] do not recommend APMM as a first-line treatment but prefer meniscal repair or conservative treatment instead. It might, however, serve as an alternative when the latter two treatment options are not applicable (complex tears, tears with high degree of degeneration, flap tears or nonreducible bucket handle tears) or when response to meniscal repair or conservative treatment has been unsatisfactory.

A significant subset (6%–25%) of partial meniscectomy patients experience persistent or recurrent pain within 1–2 years after APMM [13, 49], also known as the postmeniscectomy syndrome. These patients typically suffer from dull and nagging pain in the operated knee compartment, often accompanied by transient joint effusions [37].

Several studies have established common risk factors for inferior APMM outcome [42], including age, obesity, cartilage status, coronal malalignment [48] and the extent of the meniscectomy [14]. These risk factors are all related to a mismatch between the applied load (obesity, activity level, coronal malalignment) and reduced resilience to resist and endure that load (meniscus dysfunction or cartilage loss).

An often overlooked but potentially significant risk factor for medial postmeniscectomy syndrome (MPMS) is three-dimensional (3D) knee morphology. Previous publications on medial knee compartment morphology indicated a potential link between a small medial femoral condyle and early degeneration of the medial meniscus [17, 44]. The relationship between specific bony knee morphology variations and certain pathologies such as cruciate ligament lesions [15] and patellar instability [20] has already been demonstrated. Although bony morphology is nonmodifiable, it is of great importance to detect and acknowledge this factor, as it may have an influence on surgery outcomes [36].

A commonly used method to analyse bone morphology is measuring several anatomical landmark-based distances and angles, either on the 3D bone models or directly on the medical images. While very straightforward and easy to visualise, this approach suffers from some limitations. First, it only captures information at discrete, predefined anatomical landmarks, thereby neglecting the complexity of shape variation patterns over the entire bone surface. Second, the choice of morphological parameters or measurements is subjective and might be prone to a selection bias, potentially overlooking essential morphological features.

Statistical shape modelling offers a powerful alternative that overcomes these limitations. By analysing large data sets of 3D bone models (e.g., from magnetic resonance imaging [MRI] scans), statistical shape modelling involves the creation of a smart shape atlas that captures the average bone shape and its main modes of shape variation in a data-driven way. It eliminates the need for subjectively chosen landmarks and instead analyses the entire articular bone surface at once. As a result, it will lead to a deeper understanding of the complex interplay between distinct morphological features in the context of APMM outcome.

Statistical shape modelling has been around for several years [11] but only recently found its way to the field of orthopaedics [10, 19, 29, 32]. In the present study, it allows to quantitatively compare the femoral and tibial bone shapes between two groups of meniscectomy patients and to extract potential morphological predictors for clinical response to APMM.

The purpose of this study was to investigate if adult APMM patients who develop pain symptoms (MPMS) demonstrate different bony knee morphology, compared to APMM patients who do not develop pain symptoms, within a follow-up of 2 years after APMM. Based on our previous findings [17, 44], related to a small medial femoral condyle morphotype as a risk factor in the multifactorial process of medial compartment knee pain, we hypothesise the MPMS knees to have a smaller medial femoral condyle. Finally, this study aimed to evaluate a predictive model for APMM outcome with bony morphology as predictor variables.

MATERIALS AND METHODS

This study is a multicentre, retrospective case–control study. Three high-volume orthopaedic centres specialised in knee pathology from Antwerp, Milan and Regensburg participated in this study. Institutional Review Board approval was obtained from all local ethical committees (Comité voor medische ethiek AZ Monica and UZA: study B300201941743, Ethikkommission an der Universität Regensburg: reference 19-1621-101, IRCCS Istituto Clinico Humanitas: study authorisation n. 2515), and informed consent was obtained from all patients prior to their inclusion.

Patient selection and study design

Patients were eligible for the study if they were between 18 and 70 years old and had a primary medial meniscus lesion, for which meniscal repair or conservative treatment was not applicable, and, hence an APMM was indicated and performed by an expert surgeon ($N = 844$). Predefined exclusion criteria were unavailable preoperative MRI, inability to communicate, an unstable knee (International Knee Documentation Committee [IKDC] grade C or D), patellar instability or trochlear dysplasia, limited knee range of motion (IKDC grade C or D), cartilage lesions (grade IV and larger than 2 cm, nonfocal), coronal malalignment (as judged clinically), concomitant discoid meniscus, morbid obesity (body mass index [BMI] > 35), a history of

meniscus repair or major lower limb surgery prior to the meniscectomy, septic or rheumatoid arthritis, neurological disorders, posterior cruciate ligament repair or reconstruction, insufficiency fractures or avascular necrosis, plica syndrome or less than 2 mm intact medial meniscal rim left intraoperatively. Finally, 443 patients were eligible after screening of their hospital records, of which 42 had an MRI of insufficient quality (movement artefacts or slice thickness > 4 mm) and 161 did not consent study participation or did not complete the Knee injury and Osteoarthritis Outcome Score (KOOS) questionnaire.

As pain is the primary symptom for diagnosis of the postmeniscectomy syndrome, the KOOS pain subscore [40, 41] was used to split the APMM patients into two groups: a first group who showed a good clinical response to APMM (further referred to as R group) and a second group who developed MPMS (further referred to as MPMS group). A power analysis defined the required sample size as 120 patients per group. The KOOS pain score threshold for stratification of the subgroups was set at 75, based on the patient acceptable symptom state, as calculated by Agarwalla et al. [2]. The R group included 120 patients with a KOOS pain score > 75 and the MPMS group included 120 patients with a failed clinical outcome, defined as KOOS pain score ≤ 75. The predefined total study sample size ($N = 240$) was considered adequate to build a robust statistical shape model (SSM) covering population variance [5].

The patient selection procedure is summarised in the CONSORT diagram in Figure 1. All patients were

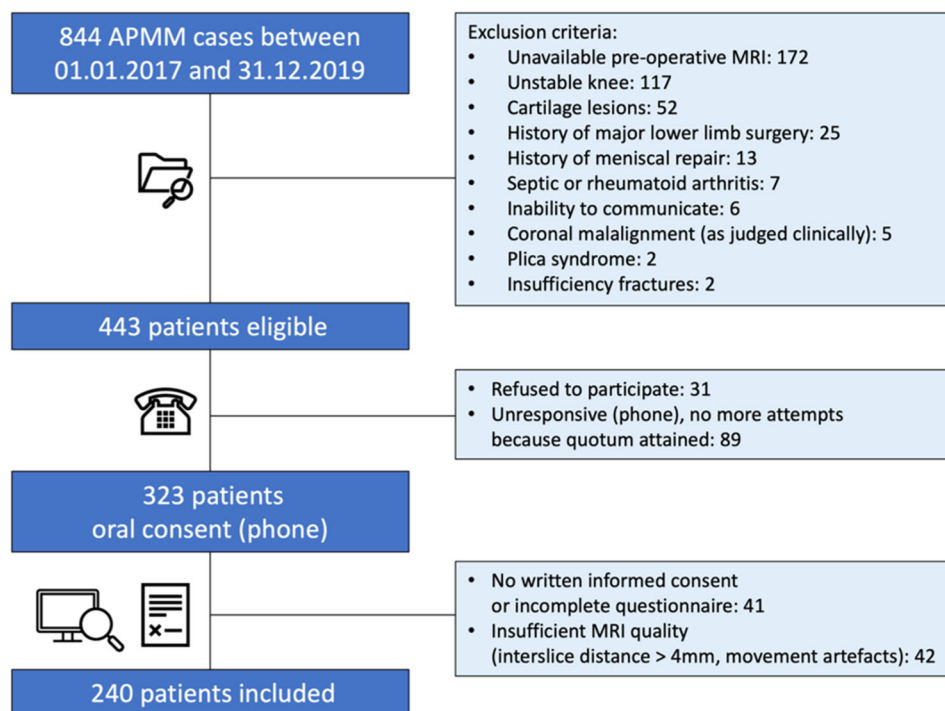


FIGURE 1 Consolidated Standards of Reporting Trials flow diagram for subject enrolment procedure. All subjects underwent an arthroscopic partial medial meniscectomy (APMM). MRI, magnetic resonance imaging.

first approached by phone. Documents (informed consent and KOOS questionnaire) were sent following oral consent to participate into the study. Upon attaining the predefined sample size in one group ($n = 120$), no additional patients were included in that group, and attempts to contact patients with incomplete KOOS questionnaires or informed consent were stopped when both groups were complete ($n = 240$).

Data collection

Imaging, demographic and clinical data were collected. The imaging data consisted of the preoperative MRI scans used for diagnosis of the meniscal lesion and was extracted from the hospital picture archiving and communication system (PACS). MRI scans were evaluated by one experienced researcher for motion artefacts and slice thickness < 4 mm. A typical preoperative MRI (1.5 or 3T) protocol included the following sequences: coronal T1-weighted (3.5 mm slice thickness, 0.7×0.7 mm in-plane resolution), coronal proton density (PD)-weighted (3.5 mm slice thickness, 0.5×0.5 mm in-plane resolution), sagittal PD (3.5 mm slice thickness, 0.5×0.5 mm in-plane resolution) and axial T2- or intermediate-weighted (3 mm slice thickness, 0.5×0.5 mm in-plane resolution) images. Collected demographic and clinical data included patient sex, age, weight and height. BMI was calculated from patient weight and height as follows: patient weight (kg) divided by the square patient height (m). Cartilage status (modified Outerbridge classification [3]) was extracted from the surgery reports and verified on the preoperative MRI scans. The KOOS questionnaire [41] at 2 years of follow-up served as a patient-reported outcome measure to evaluate response to treatment (RTT).

Generation of 3D bone models

Preoperative MRI scans were extracted from the PACS system in DICOM format and loaded into Mimics 23.0 (Materialise NV). Following the standard knee scan protocols, sequences in the three perpendicular anatomical planes were available. Using at least two MRI sequences with a perpendicular acquisition plane, distal femur and proximal tibia were segmented into two separate 3D models, each of them consisting of bone and cartilage united. The projected contours of the resulting 3D models were doublechecked on all available sequences and fine-tuned manually using the 'Contour edit' tool of the software package. 3D models of the distal femur and proximal tibia were then saved as triangular meshes and further used to perform the morphological analysis.

SSM: Data-driven morphology description

In total, three SSMs were built from the 3D bone models: one separate SSM for the isolated distal femur, one SSM for the isolated proximal tibia [12] and a combined SSM of the tibiofemoral joint in full extension following the methodology described by Audenaert et al. [4].

The first step in building an SSM is the establishment of anatomical correspondences between the patient-specific bone shapes. This involves the automatic identification and matching of the same anatomical landmarks and regions across the different bone shapes in the data set. Practically, this was achieved through an iterative process of rigid and elastic deformations as described and validated by Danckaers et al. [12]. Briefly, a template triangular bone mesh of the distal femur or proximal tibia was gradually deformed to the bone shape of the patients, resulting in a mesh with a dense set of pseudo-landmarks that share a consistent anatomical meaning across all patients. Next, all patient bone shapes were rigidly aligned (rotations, translations) to the same position by minimising the sum of distances between all corresponding points. To reduce any variability induced by the MRI scan field of view, only the distal portion of the femur and proximal portion of the tibia was selected for further analysis (blue region in Figure 2).

The previously established anatomical correspondences ensure that the same anatomical region is selected for all patients.

A custom Python script was written to construct the SSM. The mean bone shape was calculated, and principal component analysis (PCA) resulted in the main modes of shape variation [11]. PCA is a commonly used mathematical method for dimensionality reduction, which transforms the original variables (numerous 3D model point coordinates x , y and z for each bone shape) linearly into a set of new variables

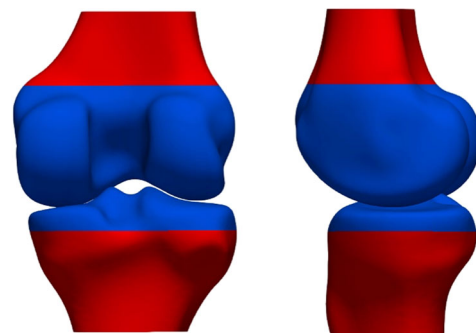


FIGURE 2 Definition of the distal femur and proximal tibia to be included in the shape analysis (blue region). The red surface region was neglected in the shape analysis. Left: posterior view. Right: medial view.

(confined number of modes of shape variation), ordered by decreasing magnitude (explained shape variance). Together, the mean bone shape and the modes of shape variation define the SSM, and they can describe any shape of the same nature as a weighted sum of those modes. The weight factors for each mode of shape variation are then called principal component (PC) weights. Given the SSM, the PC weights for each mode of shape variation are then used to characterise the patient-specific bone morphology. The SSM construction is summarised and illustrated in Figure 3.

In the combined SSM, the adopted method of Audenaert et al. [4] realigned the individual bones to an average (neutral) relative position before inclusion in the SSM, thereby removing any potential relative positional information (e.g., induced by patient positioning in the scanner). Without this realignment, any positional variation (e.g., flexion/extension, varus/valgus, internal/external rotation) would also be captured in the main modes of shape variation, thereby resulting in a less compact SSM.

For all three SSMs in this study, the modes of shape variation were defined on the complete data set of 240 knees. Model compactness and generalisation were evaluated as performance metrics for all three SSMs [5].

Model compactness

Compact shape models can describe any new shape instance with as little modes of shape variation as possible [16]. SSM compactness is described as the cumulative explained variance in the function of the number of modes. The higher this value, the fewer modes are needed for the SSM to describe shape variation at the population level and increase model performance. A cumulative explained variance ratio of more than 98% was aimed for when choosing the appropriate number of modes.

Model generalisability

For matters of future clinical applications, the SSM should generalise to unseen shapes of the same nature [16]. That is, it should be able to describe unseen bone shapes to a certain level of accuracy. Repeated leave-one-out cross-validation experiments were performed in order to assess this capability for an increasing number of modes of shape variation. The generalisation metric was then defined as the average description error (root mean square error [RMSE]) over all experiments.

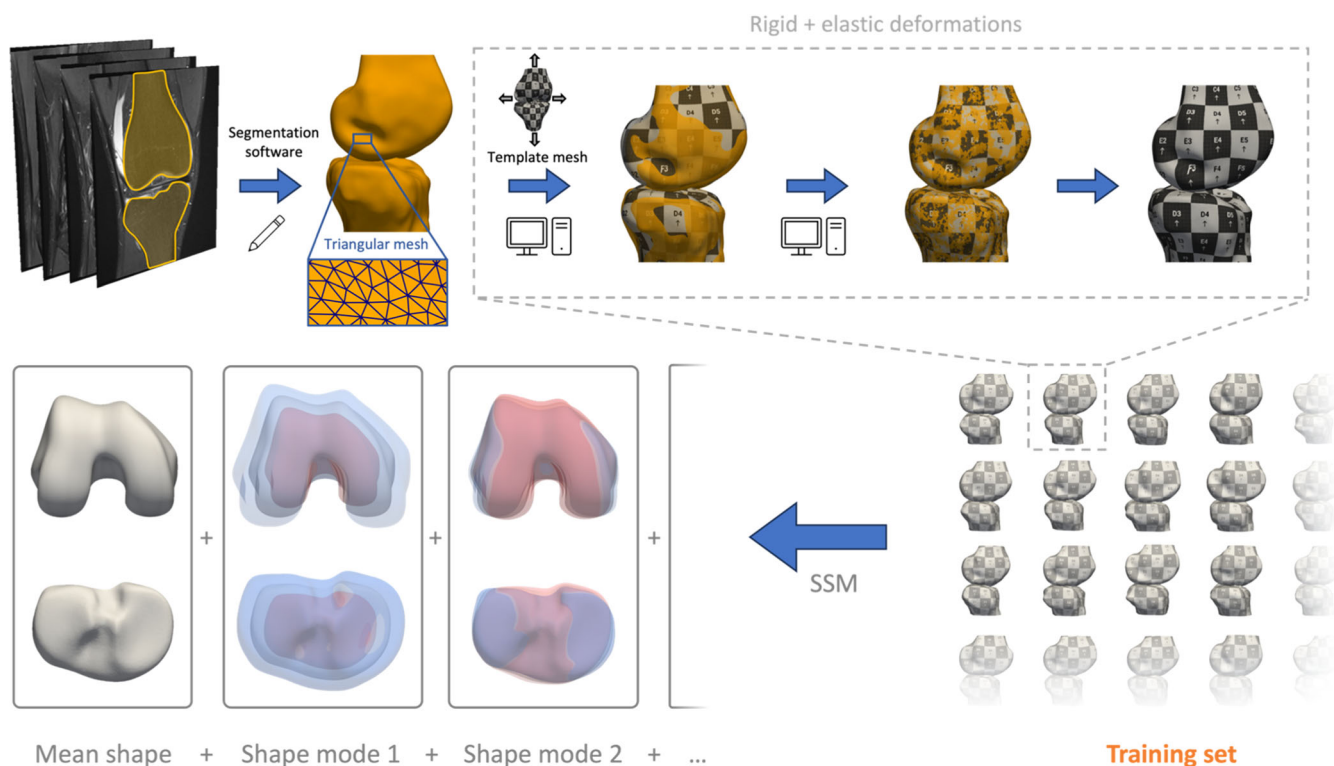


FIGURE 3 Starting from the medical images, three-dimensional models were manually created in the segmentation software. Next, anatomical correspondences are computed by rigidly and elastically deforming a template mesh (visualised with checker pattern). These deformed template meshes (=training set) are then further used to construct the statistical shape model (SSM).

SSM in relation to clinical data and RTT

PC weights for the specific modes of shape variation were calculated for all patients in both R and MPMS groups. The PC weights for the first three modes of shape variation were then compared between the R and MPMS group, and a physical meaning was assigned to those modes (results section Knee morphology comparison between R and MPMS group). In the next step, correlations between demographic, clinical and morphology variables (PC weights) were assessed (section Correlation analysis between demographic, clinical and morphology variables). Finally, a predictive algorithm for RTT based on knee morphology was trained and evaluated (section Prediction of RTT based on knee morphology).

Statistical analysis

All statistical analyses were performed in RStudio (Version 2022.07.0.1; R Studio, PBC) and R (version 4.2.1; R Foundation). Training and cross-validation of the predictive algorithm were performed in Python (open-source library scikit-learn v1.1.2) [34]. Statistical significance level was defined at $p < 0.05$.

Study population

Descriptive statistics for the continuous variables patient age, weight, height and BMI included mean and standard deviation, while the categorical variable patient sex was reported as count and percentage. Differences in distributions between the R and MPMS groups were tested by the two-sided student t test for the continuous variables, Fischer's exact test for the variable sex and a χ^2 test of independence for cartilage status.

Knee morphology comparison between R and MPMS group

PC weights distributions for the first three modes of shape variation were compared between the R and MPMS groups using Welch's unequal variances t test.

Correlation analysis

Pearson correlation coefficients were calculated between the following variables: patient sex (recoded as 0 for female and 1 for male), patient age, patient length, patient weight, KOOS and the PC weights of the first three modes of shape variation for all three SSM. Statistical significant Pearson correlation coefficients were reported in a correlation matrix.

Prediction of RTT

The predictive value of PC weights for RTT (recoded as 1 for the R group and 0 for the MPMS group) was assessed. Prediction of RTT was performed by means of logistic regression on the PC weights in a leave-one-out cross-validation experiment. Sensitivity and specificity were calculated for the detection of both RTT and MPMS [39]. In addition, the area under the curve for the receiver operating characteristic curve [39] (AUC-ROC) was calculated. A bootstrapping experiment with 1000 iterations was performed to calculate 95% confidence intervals (CIs).

RESULTS

Study population

There were no significant differences between the R and MPMS groups in patient sex, patient age, patient weight, patient height and BMI distributions (Table 1). Cartilage status according to the modified Outerbridge scale (intraoperative assessment) was not significantly different between the two groups for all regions. The KOOS and all of its subscales were significantly different ($p < 0.001$ for all KOOS subscales, Figure 4).

Knee morphology comparison between R and MPMS groups

Distal femur

Regarding compactness, the SSM of the distal femur captured 98.0% of the shape variance in the first 36 modes of shape variation (model compactness). Generalisation error to unseen distal femur shapes in leave-one-out experiments was on average 0.30 mm (RMSE). More detailed performance metrics of the SSMs can be found in Supporting Information.

The first mode of shape variation is the 3D size of the distal femur (Figure 5, left column). Distal femora of the MPMS group were significantly smaller than those in the R group ($p < 0.001$). The second mode of shape variation (Figure 5, middle column) captured the mediolateral (ML) intercondylar notch width. The MPMS group had a significantly wider intercondylar notch ($p < 0.001$). The third mode of shape (Figure 5, right column) variation encompassed the ML width of the medial femoral condyle and anteroposterior (AP) length of both femoral condyles. MPMS knees had a significantly smaller ML medial femoral condyle and larger AP femoral condyles ($p < 0.001$). Together, these three modes of shape variation accounted for 86.7% of the total femoral shape variance.

TABLE 1 Count and percentage for patient sex and cartilage lesion classification (modified Outerbridge), mean \pm SD for variables patient age, patient weight, patient height and BMI in both R and MPMS groups.

	R group	MPMS group	p Value
Patient sex [number (%)] ^a	29 (24.2) females, 91 (75.8) males	36 (30.0) females, 84 (70.0) males	n.s.
Patient age (years) ^b	50.7 \pm 12.1	52.7 \pm 10.5	n.s.
Patient weight (kg) ^b	82.0 \pm 15.1	82.2 \pm 14.4	n.s.
Patient height (cm) ^b	177.2 \pm 8.6	175.2 \pm 9.6	n.s.
BMI (kg/m ²) ^b	26.0 \pm 3.8	26.7 \pm 3.4	n.s.
Cartilage lesion classification [number (%)] ^c			
Medial femoral condyle			
Grade 0–I	47 (39.2)	37 (31.4)	n.s.
Grade II	50 (41.7)	43 (36.4)	
Grade III	17 (14.1)	32 (27.1)	
Grade IV focal	6 (5.0)	6 (5.1)	
Medial tibial plateau			
Grade 0–I	56 (46.7)	57 (48.3)	n.s.
Grade II	50 (41.6)	46 (39.0)	
Grade III	11 (9.2)	13 (11.0)	
Grade IV focal	3 (2.5)	2 (1.7)	
Lateral femoral condyle			
Grade 0–I	71 (59.2)	85 (72.0)	n.s.
Grade II	47 (39.2)	29 (24.6)	
Grade III	1 (0.8)	1 (0.9)	
Grade IV focal	1 (0.8)	3 (2.5)	
Lateral tibial plateau			
Grade 0–I	70 (58.3)	85 (72.0)	n.s.
Grade II	47 (39.2)	29 (24.6)	
Grade III	1 (0.8)	2 (1.7)	
Grade IV focal	2 (1.7)	2 (1.7)	

Abbreviations: BMI, body mass index; MPMS, medial postmeniscectomy syndrome; n.s., nonsignificant.

^aFischer exact test.

^bTwo-sided student *t* test.

^c χ^2 test of independence.

Proximal tibia

The SSM of the proximal tibia described 98.1% of the shape variance in the first 37 modes of shape variation that. Leave-one-out experiments resulted in an average generalisability error of 0.25 mm RMSE.

The first mode of shape variation (Figure 6, left column) in the proximal tibia was 3D size. The MPMS group consisted of significantly smaller tibial plateaus ($p=0.005$). The second mode of shape variation (Figure 6, middle column) included ML width of the

tibial plateau and interspine distance, as well as tibial spine height variation. The MPMS group had a significantly wider interspine distance and lower tibial spines ($p<0.001$). The third mode of shape variation (Figure 6, right column) included the AP length of the tibial plateau and the sagittal concavity of the medial tibial plateau. A small difference was observed between the R and MPMS groups for this mode of shape variation ($p=0.01$), where tibial plateaus from the MPMS group had a more pronounced ML width relative to their AP depth and a less concave (sagittal plane) medial tibial plateau. Together, these three

modes of shape variation explained 83.7% of the total tibial shape variance.

Tibiofemoral joint (combined shape model in neutral position)

The combined SSM of femur and tibia together captured 98.0% of the variance in 46 modes of shape variation as a measure of the model compactness. This

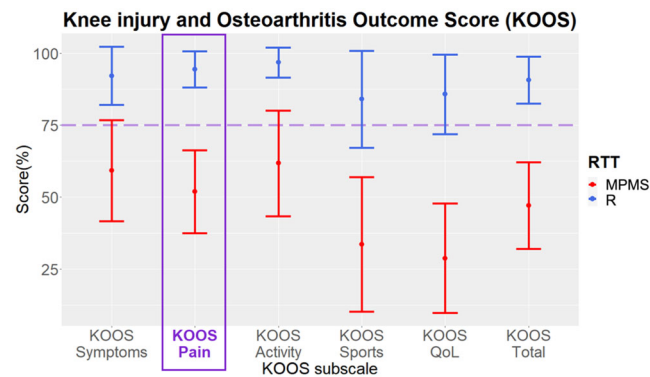


FIGURE 4 Mean \pm standard deviation of all Knee injury and Osteoarthritis Outcome Score (KOOS) subscales for both medial postmeniscectomy syndrome group (MPMS) (red) and response to treatment group (R) (blue) groups. RTT, response to treatment.

corresponded to a generalisation error of 0.34 mm in the leave-one-out experiments.

The main mode of shape variation (Figure 7, left column) in the tibiofemoral joint was size and accounted for 83.4% of the total shape variance. The distribution of the PC weights was significantly shifted towards smaller knees in the MPMS group ($p < 0.001$). The second mode of shape variation (Figure 7, middle column) described the intercondylar ML notch width and tibial interspine distance. A wider femoral intercondylar notch and larger tibial interspine distance were observed in the MPMS group ($p < 0.001$). The third mode of shape variation (Figure 7, right column) included the ML width of the medial femoral condyle and the height of the tibial spines. A significantly smaller medial femoral condyle and less pronounced tibial spines were observed in the MPMS knees ($p < 0.001$). Together, these three modes of shape variation described 88.2% of the total tibiofemoral shape variance.

Correlation analysis between demographic, clinical and knee morphology variables

Statistical significant Pearson correlation coefficients (R^2) were summarised in a correlation matrix (Table 2)

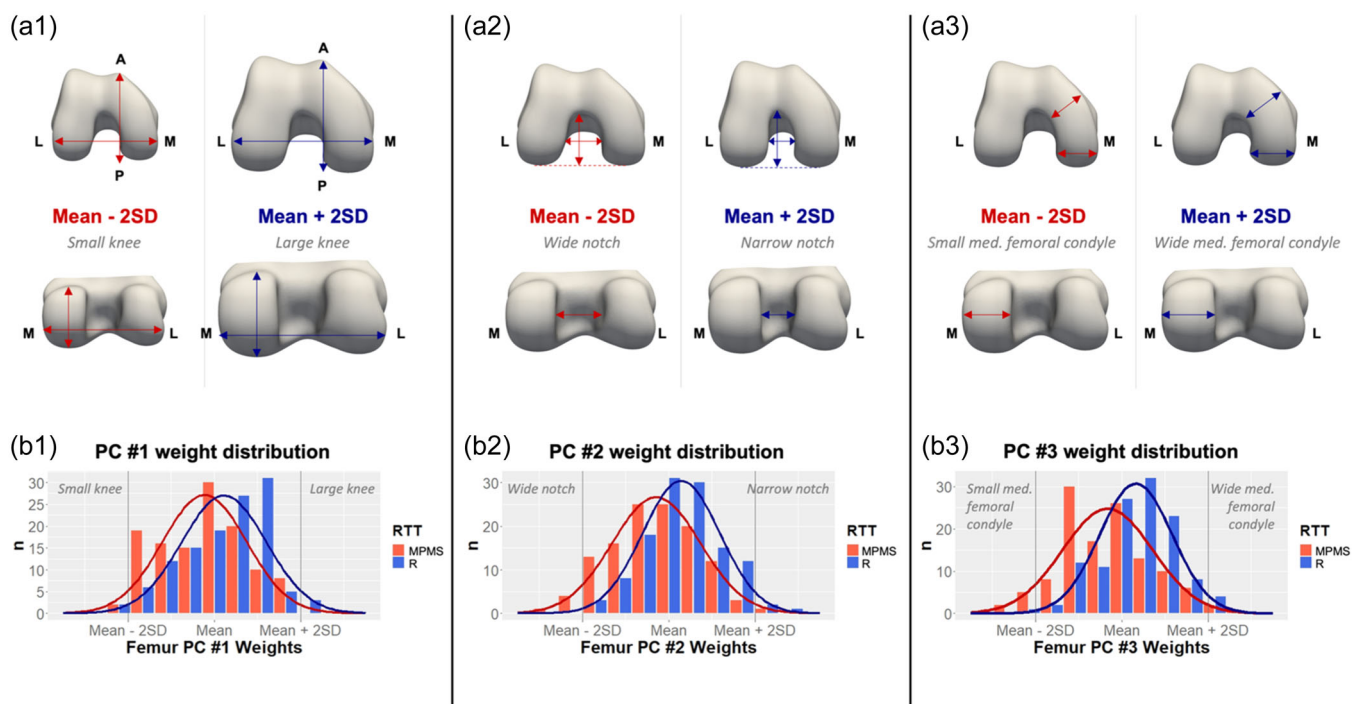


FIGURE 5 (a1–a3) First three modes of shape variation in distal femur: (top) inferior view, (bottom) posterior view. (b1–b3) Histogram of principal component (PC) weights distribution for the first three modes of shape variation in medial postmeniscectomy syndrome group (red) and response to treatment group (R) (blue) group. A, anterior; P, posterior; L, lateral; M, medial; MPMS, medial postmeniscectomy syndrome group; n, number of cases; RTT, response to treatment; SD, standard deviations.

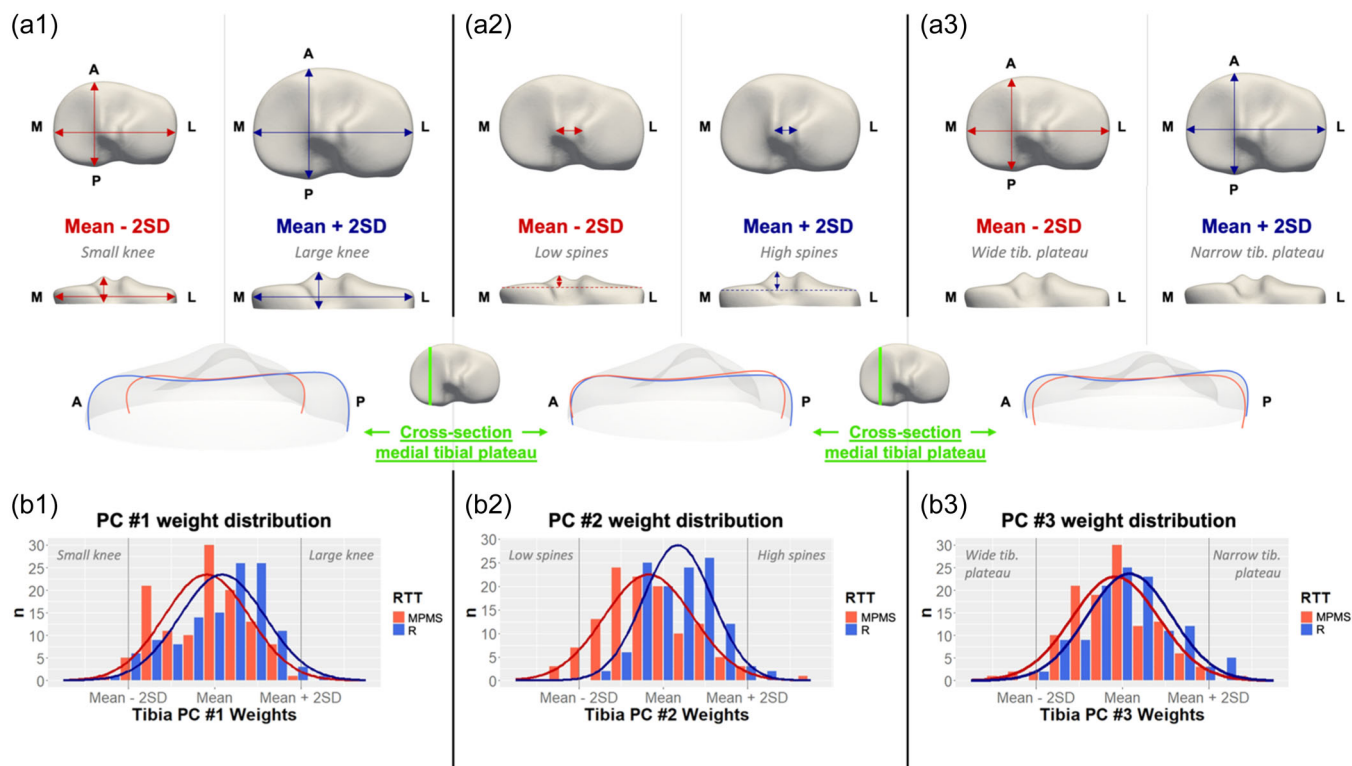


FIGURE 6 (a1–a3) First three modes of shape variation in proximal tibia: (top) superior view, (middle) posterior view, (bottom) cross-sectional medial view of the medial tibial plateau. (b1–b3) Histogram of principal component (PC) weights distribution for the first three modes of shape variation in medial postmeniscectomy syndrome group (MPMS) (red) and response to treatment group (R) (blue) group. A, anterior; L, lateral, M, medial; n , number of cases, P, posterior; RTT, response to treatment; SD, standard deviations.

for the demographic, clinical and morphological variables of the distal femur, proximal tibia and tibiofemoral joint. RTT was encoded as 0 for the MPMS group and 1 for the R group. RTT was strongly positively correlated with all KOOS subscores ($p < 0.001$). For all three SSMs (femur, tibia and tibiofemoral joint), the PC weights of the first three modes of shape variation were all very weakly to weakly (R^2 between 0.16 and 0.37) correlated with RTT ($p \leq 0.01$). None of the demographic or clinical variables were correlated with RTT.

Patient sex, length and weight were strongly positively correlated (R^2 between 0.62 and 0.80) with the first mode of shape variation (3D size) for all three SSMs ($p < 0.001$). Patient sex showed a very weak and weak negative correlation with the second mode of shape variation (femoral notch width and tibial interspine distance) from, respectively, the SSM of the proximal tibia ($R^2 = -0.13$, $p = 0.047$) and the SSM of distal femur and tibiofemoral joint (R^2 between -0.21 and 0.20 , $p < 0.002$).

Prediction of RTT based on knee morphology

Distal femur morphology is an independent predictor for RTT. Solely based on the distal femur PC weights,

MPMS was predicted with a sensitivity of 74.8% (95% CI: 74.3%–75.3%) and a specificity of 80.3% (95% CI: 79.8%–80.8%). AUC-ROC (Figure 8, yellow curve) for this classifier was 0.827 (95% CI: 0.824–0.830).

The predictive logistic regression algorithm with proximal tibia PC weights as input, identified MPMS in a leave-one-out cross-validation experiment with a sensitivity of 74.7% (95% CI: 74.2%–75.2%) and a specificity of 78.5% (95% CI: 78.0%–79.0%). AUC for the ROC curve (Figure 8, blue curve) was 0.836 (95% CI: 0.833–0.839) for this classifier based on proximal tibia morphology.

Tibiofemoral joint morphology predicted MPMS with a sensitivity of 74.9% (95% CI: 74.4%–75.4%) and a specificity of 81.0% (95% CI: 80.6%–81.5%) in a leave-one-out cross-validation experiment. AUC-ROC was 0.840 (95% CI: 0.837–0.843) for this tibiofemoral joint morphology-based classifier. The ROC curve for the classifier using a set of tibiofemoral joint shape features is shown in Figure 8 (green curve).

DISCUSSION

This study unveils for the first time bony knee morphological differences between responders to APMM and MPMS patients: a smaller overall size of

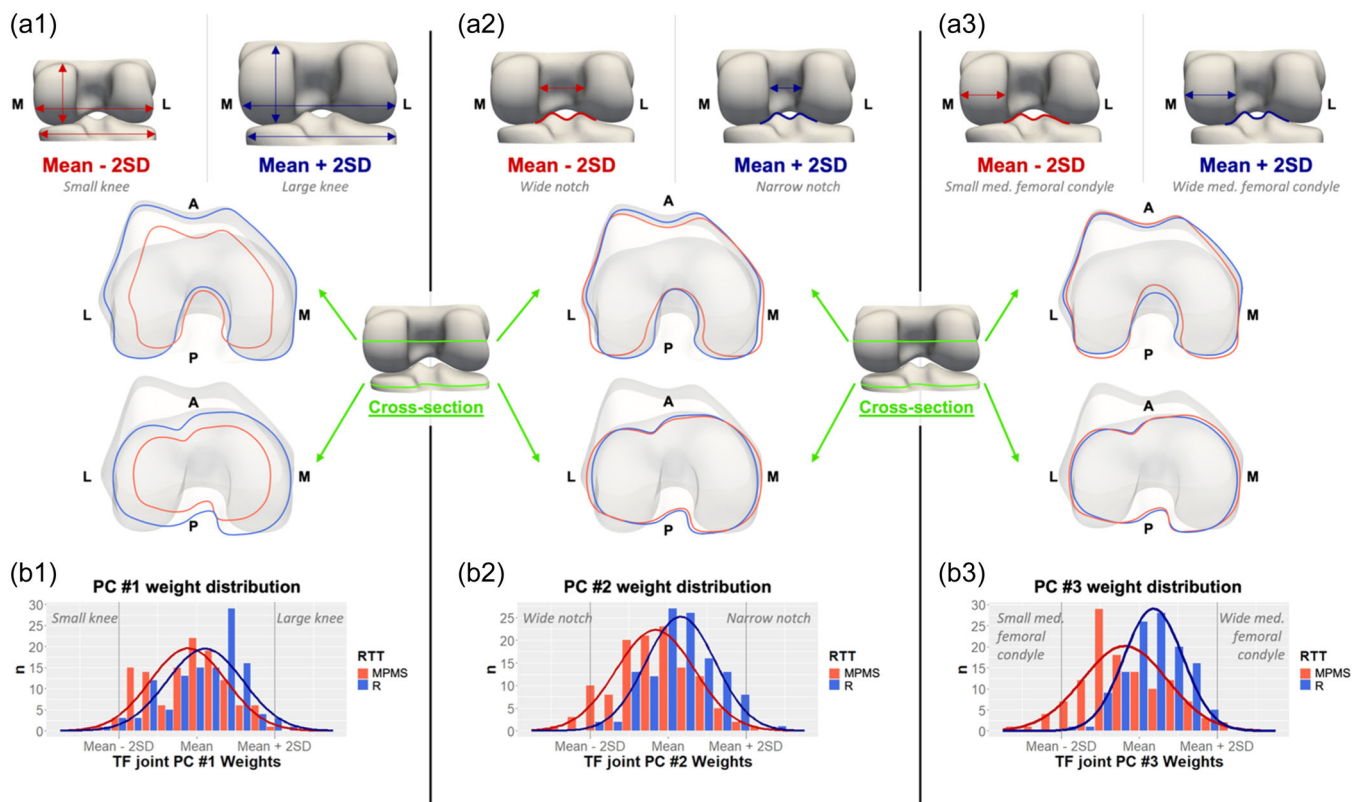


FIGURE 7 (a1–aA3) First three modes of shape variation in tibiofemoral joint: (top) posterior view, (middle) inferior view cross-sections of distal femur, (bottom) inferior view cross-sections of proximal tibia. (b1–b3) Histogram of principal component (PC) weights distribution for the first three modes of shape variation in medial postmeniscectomy syndrome group (MPMS) (red) and response to treatment group (R) (blue) group. A, anterior; L, lateral, M, medial; n , number of cases; P, posterior; RTT, response to treatment; SD, standard deviations.

the knee, a wider intercondylar notch and a smaller medial femoral condyle were the main morphological variations identified in MPMS knees. Moreover, as a second key finding in this study, morphology-based predictive models demonstrated a sensitivity of more than 75% and a specificity surpassing 80% in anticipating the outcome of APMM.

Based on these findings, a biomechanical mechanism is hypothesised to explain the main differentiating mode of shape variation between responders to APMM and MPMS. While often excluded or filtered out in statistical shape analysis, a significant difference in knee size was observed between the R and MPMS group knees for the three SSMs: isolated femur, isolated tibia and combined in the tibiofemoral joint. The knees from the MPMS group patients were significantly smaller than their counterparts in the R group, in contrast with no differences in patient length, weight and BMI between both groups. A smaller knee implicates a smaller articular contact surface area. In biomechanics, pressure is defined as force per unit area of surface. Therefore, a smaller knee loaded with a similar body weight is subject to higher pressure. Different studies already established increased contact

pressure as a central driver in progressive knee degeneration [30, 33].

To the authors' knowledge, this is the largest 3D knee morphology database of post-meniscectomized patients, consisting of imaging, demographic and clinical (incl. patient-reported outcome measure) data at 2 years postoperatively. Similar techniques based on statistical shape modelling have already been applied on other pathologies, for example, for automatic staging of trochlear dysplasia [10] or identifying morphological bone variations linked to scaphoid fractures [8].

Previously, our pilot study on medial compartment degeneration already identified the small medial femoral condyle morphotype [17] and its potential association with early medial compartment degeneration. Several *in silico* and *in vitro* studies have confirmed the load-distributing function of the meniscus, as well as the increase in cartilage peak stress after partial meniscectomy [43]. The smaller contact surface area in the small medial femoral condyle morphotype could already imply a higher peak stress compared to a wide medial femoral condyle knee. By further reducing the contact surface area, meniscus functional loss by

TABLE 2 Correlation matrix of demographic, clinical, PROM- and SSM-derived variables.

	RTT	Sex	Age	Length	Weight	BMI	KOOS symptoms	KOOS pain	KOOS activity	KOOS sports	KOOS QoL	KOOS total	Femur PC #1 weights	Femur PC #2 weights	Femur PC #3 weights	Tibia PC #1 weights	Tibia PC #2 weights	Tibia PC #3 weights	Tibiofemoral joint PC #1 weights	Tibiofemoral joint PC #2 weights	Tibiofemoral joint PC #3 weights
RTT	1.00						0.74	0.87	0.78	0.77	0.85	0.86	0.23	0.29	0.33	0.18	0.35	0.16	0.22	0.32	0.37
Sex	1.00	1.00			0.55	0.21				0.20		0.14	0.77	-0.21		0.79	-0.13		0.78	-0.20	
Age		1.00	1.00		-0.32					-0.15		-0.13	-0.21	-0.23		-0.19			-0.20	-0.22	
Length			1.00	1.00	0.67	0.14	0.17	0.14		0.25		0.17	0.80			0.79			0.80		
Weight				1.00	1.00	0.82							0.63			0.62			0.63		
BMI					1.00	1.00			-0.13				0.24			0.24			0.24		
KOOS symptoms							1.00	0.84	0.82	0.76	0.81	0.90	0.26	0.21	0.31	0.23	0.23		0.25	0.24	0.32
KOOS pain								1.00	0.93	0.82	0.90	0.96	0.26	0.28	0.35	0.21	0.31	0.15	0.25	0.31	0.38
KOOS activity									1.00	0.82	0.86	0.94	0.25	0.26	0.32	0.22	0.31	0.14	0.24	0.29	0.35
KOOS sports										1.00	0.83	0.92	0.33	0.19	0.27	0.31	0.25		0.33	0.22	0.29
KOOS QoL											1.00	0.95	0.24	0.27	0.35	0.19	0.36	0.17	0.23	0.31	0.40
KOOS total												1.00	0.29	0.26	0.34	0.25	0.32	0.15	0.28	0.29	0.37
Femur PC #1 weights													1.00			0.98			1.00		
Femur PC #2 weights														1.00			0.32	0.46		0.99	
Femur PC #3 weights															1.00		0.16				0.93
Tibia PC #1 weights																1.00			0.99		
Tibia PC #2 weights																	1.00			0.40	0.40
Tibia PC #3 weights																		1.00		0.49	-0.18
Tibiofemoral joint PC #1 weights																			1.00		

(Continues)

TABLE 2 (Continued)

RTT	Sex	Age	Length	Weight	BMI	KOOS symptoms	KOOS pain	KOOS activity	KOOS sports	KOOS QoL	KOOS total	Femur PC #1 weights	Femur PC #2 weights	Femur PC #3 weights	Tibia PC #1 weights	Tibia PC #2 weights	Tibia PC #3 weights	Tibiofemoral joint PC #1 weights	Tibiofemoral joint PC #2 weights	Tibiofemoral joint PC #3 weights			
																						1.00	
																							1.00

Note: Only significant ($p < 0.05$) Pearson R^2 correlation coefficients were plotted.

Abbreviations: BMI, body mass index; KOOS, Knee injury and Osteoarthritis Outcome Score; PC, principal component; PROM, patient-reported outcome measure; RTT, response to treatment; SSM, statistical shape model.

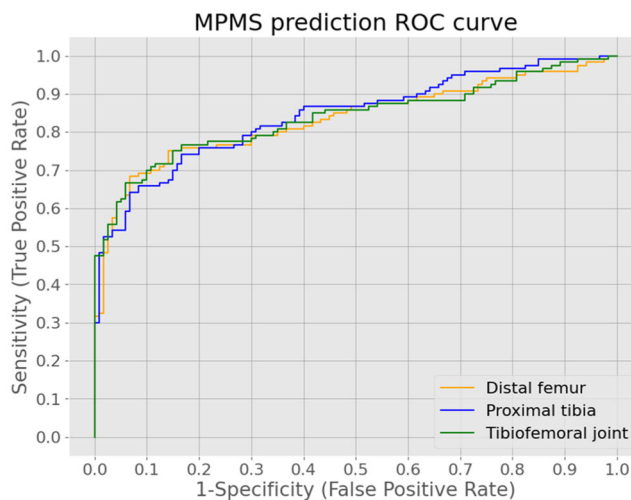


FIGURE 8 Receiver operating characteristic curves for three distinct classifiers, using a set of distal femur, proximal tibia or tibiofemoral joint shape features as predictor for medial postmeniscectomy syndrome (MPMS). ROC, receiver operating characteristic.

degeneration or APMM might additionally increase the peak stress, leading to insufficiency of the cartilage and subchondral bone to bear the load [27]. This is clinically reflected in the postmeniscectomy syndrome.

Several studies established the association between coronal alignment of the knee and pathology [22, 31]. In our study, the influence of alignment as a latent prognostic factor was minimised since all knees had a coronal alignment within the physiological range per clinical judgement. The combination of a full lower limb phenotype analysis with this confined knee morphology analysis might even result in more robust algorithms to predict APMM outcomes, irrespective of knee malalignment.

A clustering analysis by Hohlmann et al. [23] revealed no distinct morphotypes in end-stage knee osteoarthritis (OA) knees. In contrast to their conclusion, our current study found that knee shape (including size and aspect ratio) is highly correlated with patient demographics (sex, length, weight) and even APMM outcome. These contradictory findings can be explained by the fact that unsupervised clustering algorithms are typically less powerful for classification purposes. Importantly, the previous authors corrected for both size and aspect ratio, while these parameters were found to be significantly correlated to several clinical variables in the current study.

Based on SSMs, Bowes et al. created a score to quantify radiological disease progression in cases from the Osteoarthritis Initiative database [9, 28]. Tack et al. [45] extended this concept further to a set of OA biomarkers by adding traditional measurements (e.g., volume and surface area) and SSM-derived features for femoral bone, tibial bone and medial and lateral

meniscus. This set of biomarkers proved superior performance for the prediction of total knee replacement within 1 year in comparison with the bony SSM-derived features alone. The aforementioned studies support the hypothesis of bone shape as a biomarker and predictor for wear-related pathology. Indeed, the postmeniscectomy syndrome also lies in the spectrum of degenerative knee pathologies, and this current study was able to predict its onset solely based on the knee morphology.

The relevance of this work lies potentially in the health-economical aspect of medial meniscus lesion treatment [21, 49]. This is a promising first step towards a better identification of candidate patients for APMM [35]. Smarter risk definitions and patient selection in the future will result in more personalised health care [47]. Eventually, forthcoming clinical decision support systems might serve as a tool for clinicians to help achieving this aim.

The strengths of this study include the multicentre study design, the high volume of manually segmented MRI scans, as well as the unbiased methodology to describe knee morphology quantitatively. Instead of using predefined measurements, patterns of morphological variation were extracted by a robust mathematical algorithm. Furthermore, this high level of automated analysis starting from the 3D models of femur and tibia allows the analysis of even larger databases at a low marginal time cost (even zero human marginal time cost). Another strength of this unique data set is the highly homogenous group of patients and the equal distribution of collected potential latent demographic variables (patient sex, height and weight) influencing knee morphology across both R and MPMS groups. Finally, the preoperative imaging used to create the 3D models is already available for this pathology, even in a standard clinical setting.

This study shows promising results, despite some limitations. First, because of the multicentre retrospective study design, no precise data were available on possibly confounding variables such as personalised medication and rehabilitation protocol. However, the clinical centres (in Antwerp, Milan and Regensburg) have closely matched patient demographics and healthcare systems. All patients received nearly identical postoperative care, adhering to the latest clinical guidelines.

Second, during the follow-up period after APMM, no new MRI scans were performed unless clinically necessary. As a result, quantitative standardised measurements of the resected meniscal tissue could not be calculated, nor retrieved from the surgery report, and no subgroup analysis based on the presence of radiologic signs such as bone marrow oedema, osteonecrosis or meniscal re-tear could be performed.

Finally, it should be noted that only patients with a clinically normal coronal malalignment were included in

this study, per surgeon clinical assessment. In a real-world clinical protocol for meniscus lesion management, no full-leg standing radiographs, nor full-leg computerised tomography scans, are indicated for these patients. Given the retrospective nature of this study, exact coronal alignment measurements were, therefore, unavailable.

Future research includes large prospective validation studies, with additional follow-up imaging, to warrant the generalisability of the findings in this study.

In conclusion, morphological variations determine the clinical outcome of APMM in a patient population with comparable weight, height, alignment and cartilage status. More specifically, a smaller total knee size, a wider intercondylar notch and a smaller medial femoral condyle are strongly linked with postmeniscectomy syndrome. In addition, a predictive model was able to anticipate the clinical outcome of APMM at 2 years of follow-up with a sensitivity above 75% and a specificity exceeding 80%.

AUTHOR CONTRIBUTIONS

Peter Verdonk conceived of the presented idea. The concept was further thought through in cooperation with Annemieke Van Haver, Femke Danckaers, Jan Sijbers and Jonas Grammens. Kristien Vuylsteke, Jonas Grammens, Lotem Mahluf, Peter Angele, Elizaveta Kon and Peter Verdonk designed the data collection process. The computational framework was developed by Femke Danckaers and Jonas Grammens. Jonas Grammens and all members of the MEFISTO WP1 group contributed to the data collection and preprocessing of raw imaging data into accurate 3D models. Femke Danckaers and Jan Sijbers verified the analytical methods. Peter Verdonk, Peter Angele and Elizaveta Kon supervised the clinical findings of this work. All authors discussed the results and contributed to the final manuscript.

ACKNOWLEDGEMENTS

This project has received funding from the European Union's Horizon 2020 research and innovation programme under grant agreement No 814444 (MEFISTO).

MEFISTO WP1 GROUP

Maoz Shemesh and Eran Linder-Ganz (Active Implants BV, Haarlem, Netherlands); Alexander Stockmann and Girish Pattappa (Laboratory for Experimental Trauma Surgery, Department of Trauma Surgery, University Medical Center Regensburg, Regensburg, Germany); Denitsa Docheva (Department of Musculoskeletal Tissue Regeneration, Orthopaedic Clinic König-Ludwig-Haus, University of Würzburg, Germany); Gino Mestach (Antwerp Surgical Training, Anatomy and Research Centre, University of Antwerp, Antwerp, Belgium); Daniele Altomare (IRCCS Humanitas Research Hospital, Rozzano, Milan, Italy); Department

of Biomedical Sciences, Humanitas University, Pieve Emanuele, Milan, Italy).

CONFLICT OF INTEREST STATEMENT

The authors declare no conflict of interest.

DATA AVAILABILITY STATEMENT

The data sets used and/or analysed during the current study are available from the corresponding author on reasonable request.

ETHICS STATEMENT

This study was performed in line with the principles of the Declaration of Helsinki. Approval was granted by the Ethics Committee of University Hospital Antwerp (21 October 2019/No. B300201941743), University of Regensburg (11 December 2019/No. 19-1621-101) and IRCCS Istituto Clinico Humanitas (29 April 2020/No. 2515). Informed consent was obtained from all patients prior to their inclusion.

ORCID

Jonas Grammens  <http://orcid.org/0000-0002-9943-3329>

Femke Danckaers  <http://orcid.org/0000-0003-0330-2541>

Kristien Vuylsteke  <http://orcid.org/0000-0002-3328-0913>

Jan Sijbers  <http://orcid.org/0000-0003-4225-2487>

Peter Angele  <http://orcid.org/0000-0002-3190-8666>

Elizaveta Kon  <http://orcid.org/0000-0003-0649-2336>

Peter Verdonk  <http://orcid.org/0000-0001-6057-8590>

TWITTER

Jonas Grammens  @JonasGrammens

Jan Sijbers  @jansijbers

Peter Verdonk  @Profverdonk

References

- Abrams, G.D., Frank, R.M., Gupta, A.K., Harris, J.D., McCormick, F.M. & Cole, B.J. (2013) Trends in meniscus repair and meniscectomy in the United States, 2005–2011. *The American Journal of Sports Medicine*, 41(10), 2333–2339. Available from: <https://doi.org/10.1177/0363546513495641>
- Agarwalla, A., Gowd, A.K., Liu, J.N., Lalezarian, S.P., Christian, D.R., Cole, B.J. et al. (2019) Predictive factors and duration to return to sport after isolated meniscectomy. *Orthopaedic Journal of Sports Medicine*, 7(4), 232596711983794. Available from: <https://doi.org/10.1177/2325967119837940>
- Asano, H., Muneta, T., Ikeda, H., Yagishita, K., Kurihara, Y. & Sekiya, I. (2004) Arthroscopic evaluation of the articular cartilage after anterior cruciate ligament reconstruction: a short-term prospective study of 105 patients. *Arthroscopy: The Journal of Arthroscopic & Related Surgery*, 20(5), 474–481. Available from: <https://doi.org/10.1016/j.arthro.2004.03.006>
- Audenaert, E.A., Van den Eynde, J., de Almeida, D.F., Steenackers, G., Vandermeulen, D. & Claes, P. (2020) Separating positional noise from neutral alignment in multi-component statistical shape models. *Bone Reports*, 12, 100243. Available from: <https://doi.org/10.1016/j.bonr.2020.100243>
- Audenaert, E.A., Pattyn, C., Steenackers, G., De Roeck, J., Vandermeulen, D. & Claes, P. (2019) Statistical shape modeling of skeletal anatomy for sex discrimination: their training size, sexual dimorphism, and asymmetry. *Frontiers in Bioengineering and Biotechnology*, 7, 302. Available from: <https://doi.org/10.3389/fbioe.2019.00302>
- Beaufils, P., Becker, R., Kopf, S., Englund, M., Verdonk, R., Ollivier, M. et al. (2017) Surgical management of degenerative meniscus lesions: the 2016 ESSKA meniscus consensus. *Knee Surgery, Sports Traumatology, Arthroscopy*, 25(2), 335–346. Available from: <https://doi.org/10.1007/s00167-016-4407-4>
- Beaufils, P., Becker, R., Kopf, S., Matthieu, O. & Pujol, N. (2017) The knee meniscus: management of traumatic tears and degenerative lesions. *EFORT Open Reviews*, 2(5), 195–203. Available from: <https://doi.org/10.1302/2058-5241.2.160056>
- Bevers, M.S.A.M., Wyers, C.E., Daniels, A.M., Audenaert, E.A., van Kuijk, S.M.J., van Rietbergen, B. et al. (2021) Association between bone shape and the presence of a fracture in patients with a clinically suspected scaphoid fracture. *Journal of Biomechanics*, 128, 110726. Available from: <https://doi.org/10.1016/j.jbiomech.2021.110726>
- Bowes, M.A., Kacena, K., Alabas, O.A., Brett, A.D., Dube, B., Bodick, N. et al. (2021) Machine-learning, MRI bone shape and important clinical outcomes in osteoarthritis: data from the Osteoarthritis Initiative. *Annals of the Rheumatic Diseases*, 80(4), 502–508. Available from: <https://doi.org/10.1136/annrheumdis-2020-217160>
- Cerveri, P., Belfatto, A., Baroni, G. & Manzotti, A. (2018) Stacked sparse autoencoder networks and statistical shape models for automatic staging of distal femur trochlear dysplasia. *The International Journal of Medical Robotics and Computer Assisted Surgery*, 14(6), e1947. Available from: <https://doi.org/10.1002/rcs.1947>
- Cootes, T.F., Taylor, C.J., Cooper, D.H. & Graham, J. (1995) Active shape models—their training and application. *Computer Vision and Image Understanding*, 61(1), 38–59. Available from: <https://doi.org/10.1006/cviu.1995.1004>
- Danckaers, F., Huysmans, T., Lacko, D., Ledda, A., Verwulgent, S., Van Dongen, S. et al. (2014) Correspondence preserving elastic surface registration with shape model prior. *2014 22nd International Conference on Pattern Recognition IEEE*, 24–28 August 2014. New York: IEEE, pp. 2143–2148. Available from: <https://doi.org/10.1109/ICPR.2014.373>
- Drobnič, M., Ercin, E., Gamelas, J., Papacostas, E.T., Slynarski, K., Zdanowicz, U. et al. (2019) Treatment options for the symptomatic post-meniscectomy knee. *Knee Surgery, Sports Traumatology, Arthroscopy*, 27(6), 1817–1824. Available from: <https://doi.org/10.1007/s00167-019-05424-3>
- Eijgenraam, S.M., Reijman, M., Bierma-Zeinstra, S.M.A., van Yperen, D.T. & Meuffels, D.E. (2018) Can we predict the clinical outcome of arthroscopic partial meniscectomy? a systematic review. *British Journal of Sports Medicine*, 52(8), 514–521. Available from: <https://doi.org/10.1136/bjsports-2017-097836>
- Fernández-Jaén, T., López-Alcorocho, J.M., Rodríguez-Iñigo, E., Castellán, F., Hernández, J.C. & Guillén-García, P. (2015) The importance of the intercondylar notch in anterior cruciate ligament tears. *Orthopaedic Journal of Sports Medicine*, 3(8), 232596711559788. Available from: <https://doi.org/10.1177/2325967115597882>
- Goparaju, A., Csecs, I., Morris, A., Kholmovski, E., Marouche, N., Whitaker, R. et al. (2018) On the evaluation and validation of off-the-shelf statistical shape modeling tools: a clinical application. In: Reuter, M., Wachinger, C., Lombaert, H., Paniagua, B., Lüthi, M. & Egger, B. (Eds.) *Shape in medical*

- imaging*. Cham: Springer International Publishing, pp. 14–27. Available from: https://doi.org/10.1007/978-3-030-04747-4_2
17. Grammens, J., Van Haver, A., Danckaers, F., Booth, B., Sijbers, J. & Verdonk, P. (2021) Small medial femoral condyle morphotype is associated with medial compartment degeneration and distinct morphological characteristics: a comparative pilot study. *Knee Surgery, Sports Traumatology, Arthroscopy*, 29(6), 1777–1789. Available from: <https://doi.org/10.1007/s00167-020-06218-8>
 18. Hall, M.J., Schwartzman, A., Zhang, J. & Liu, X. (2017) Ambulatory surgery data from hospitals and ambulatory surgery centers: United States, 2010. *Natl Health Stat Report*
 19. Van Haver, A., Mahieu, P., Claessens, T., Li, H., Pattyn, C., Verdonk, P. et al. (2014) A statistical shape model of trochlear dysplasia of the knee. *The Knee*, 21(2), 518–523. Available from: <https://doi.org/10.1016/j.knee.2013.11.016>
 20. Van Haver, A., De Roo, K., De Beule, M., Labey, L., De Baets, P., Dejour, D. et al. (2015) The effect of trochlear dysplasia on patellofemoral biomechanics. *The American Journal of Sports Medicine*, 43(6), 1354–1361. Available from: <https://doi.org/10.1177/0363546515572143>
 21. Hershman, E.B., Jarvis, J.L., Mick, T., Dushaj, K. & Elsner, J.J. (2020) Direct treatment cost outcomes among patients with medial meniscus deficiency: results from a 24-month surveillance study. *Current Medical Research and Opinion*, 36(3), 427–437. Available from: <https://doi.org/10.1080/03007995.2020.1713073>
 22. Hirschmann, M.T., Moser, L.B., Amsler, F., Behrend, H., Leclercq, V. & Hess, S. (2019) Functional knee phenotypes: a novel classification for phenotyping the coronal lower limb alignment based on the native alignment in young non-osteoarthritic patients. *Knee Surgery, Sports Traumatology, Arthroscopy*, 27(5), 1394–1402. Available from: <https://doi.org/10.1007/s00167-019-05509-z>
 23. Hohlmann, B., Asseln, M., Xu, J. & Radermacher, K. (2022) Investigation of morphotypes of the knee using cluster analysis. *The Knee*, 35, 157–163. Available from: <https://doi.org/10.1016/j.knee.2022.03.006>
 24. Jacquet, C., Pujol, N., Pauly, V., Beauflis, P. & Ollivier, M. (2019) Analysis of the trends in arthroscopic meniscectomy and meniscus repair procedures in France from 2005 to 2017. *Orthopaedics & Traumatology, Surgery & Research: OTSR*, 105(4), 677–682. Available from: <https://doi.org/10.1016/j.otsr.2019.01.024>
 25. Katano, H., Koga, H., Ozeki, N., Otabe, K., Mizuno, M., Tomita, M. et al. (2018) Trends in isolated meniscus repair and meniscectomy in Japan, 2011–2016. *Journal of Orthopaedic Science*, 23(4), 676–681. Available from: <https://doi.org/10.1016/j.jos.2018.04.003>
 26. Kopf, S., Beauflis, P., Hirschmann, M.T., Rotigliano, N., Ollivier, M., Pereira, H. et al. (2020) Management of traumatic meniscus tears: the 2019 ESSKA meniscus consensus. *Knee Surgery, Sports Traumatology, Arthroscopy*, 28(4), 1177–1194. Available from: <https://doi.org/10.1007/s00167-020-05847-3>
 27. Lee, S.J., Aadalén, K.J., Malaviya, P., Lorenz, E.P., Hayden, J.K., Farr, J. et al. (2006) Tibiofemoral contact mechanics after serial medial meniscectomies in the human cadaveric knee. *The American Journal of Sports Medicine*, 34(8), 1334–1344. Available from: <https://doi.org/10.1177/0363546506286786>
 28. Lester, G. (2008) Clinical research in OA—the NIH Osteoarthritis Initiative. *Journal of Musculoskeletal & Neuronal Interactions*, 8(4), 313–314.
 29. Meynen, A., Matthews, H., Nauwelaers, N., Claes, P., Mulier, M. & Scheyfs, L. (2020) Accurate reconstructions of pelvic defects and discontinuities using statistical shape models. *Computer Methods in Biomechanics and Biomedical Engineering*, 23(13), 1026–1033. Available from: <https://doi.org/10.1080/10255842.2020.1784404>
 30. Mononen, M.E., Tanska, P., Isaksson, H. & Korhonen, R.K. (2018) New algorithm for simulation of proteoglycan loss and collagen degeneration in the knee joint: data from the Osteoarthritis Initiative. *Journal of Orthopaedic Research*, 36(6), 1673–1683. Available from: <https://doi.org/10.1002/jor.23811>
 31. Van Oevelen, A., Van den Borre, I., Duquesne, K., Pizurica, A., Victor, J., Nauwelaers, N. et al. (2022) Wear patterns in knee OA correlate with native limb geometry. *Frontiers in Bioengineering and Biotechnology*, 10, 1042441. Available from: <https://doi.org/10.3389/fbioe.2022.1042441>
 32. Osstyn, J., Danckaers, F., Van Haver, A., Oramas, J., Vanhees, M. & Sijbers, J. (2023) Automated virtual reduction of displaced distal radius fractures. *2023 IEEE 20th International Symposium on Biomedical Imaging (ISBI)*, 18–21 April 2023. New York: IEEE, pp. 1–4. Available from: <https://doi.org/10.1109/ISBI53787.2023.10230399>
 33. Pattappa, G., Zellner, J., Johnstone, B., Docheva, D. & Angele, P. (2019) Cells under pressure - the relationship between hydrostatic pressure and mesenchymal stem cell chondrogenesis. *European Cells and Materials*, 36, 360–381. Available from: <https://doi.org/10.22203/eCM.v037a22>
 34. Pedregosa, F., Varoquaux, G., Gramfort, A., Michel, V., Thirion, B., Grisel, O. et al. (2011) Scikit-learn: machine learning in python. *Journal of Machine Learning Research*, 12, 2825–2830.
 35. Pihl, K., Ensor, J., Peat, G., Englund, M., Lohmander, S., Jørgensen, U. et al. (2020) Wild goose chase—no predictable patient subgroups benefit from meniscal surgery: patient-reported outcomes of 641 patients 1 year after surgery. *British Journal of Sports Medicine*, 54(1), 13–22. Available from: <https://doi.org/10.1136/bjsports-2018-100321>
 36. Polamalu, S.K., Novaretti, J., Musahl, V. & Debski, R.E. (2022) Tibiofemoral bony morphology impacts the knee kinematics after anterolateral capsule injury and lateral extraarticular tenodesis differently than intact state. *Journal of Biomechanics*, 139, 110857. Available from: <https://doi.org/10.1016/j.jbiomech.2021.110857>
 37. Rao, A.J., Erickson, B.J., Cvetanovich, G.L., Yanke, A.B., Bach, B.R. & Cole, B.J. (2015) The meniscus-deficient knee. *Orthopaedic Journal of Sports Medicine*, 3(10), 232596711561138. Available from: <https://doi.org/10.1177/2325967115611386>
 38. Reito, A., Harris, I.A. & Karjalainen, T. (2021) Arthroscopic partial meniscectomy: did it ever work? *Acta Orthopaedica*, 93, 1–10. Available from: <https://doi.org/10.1080/17453674.2021.1979793>
 39. Riffenburgh, R.H. & Gillen, D.L. (Eds.) (2020) Risks, odds, and receiver operating characteristic curves. *Statistics in medicine*. Cambridge, Massachusetts: Academic Press, pp. 215–238. Available from: <https://doi.org/10.1016/B978-0-12-815328-4.00010-3>
 40. Roos, E.M. & Lohmander, L.S. (2003) The Knee injury and Osteoarthritis Outcome Score (KOOS): from joint injury to osteoarthritis. *Health and Quality of Life Outcomes*, 1(1), 64. Available from: <https://doi.org/10.1186/1477-7525-1-64>
 41. Roos, E.M., Roos, H.P., Lohmander, L.S., Ekdahl, C. & Beynnon, B.D. (1998) Knee Injury and Osteoarthritis Outcome Score (KOOS)—development of a self-administered outcome measure. *Journal of Orthopaedic & Sports Physical Therapy*, 28(2), 88–96. Available from: <https://doi.org/10.2519/jospt.1998.28.2.88>
 42. Salata, M.J., Gibbs, A.E. & Sekiya, J.K. (2010) A systematic review of clinical outcomes in patients undergoing meniscectomy. *The American Journal of Sports Medicine*, 38(9), 1907–1916. Available from: <https://doi.org/10.1177/0363546510370196>
 43. Sukopp, M., Schall, F., Hacker, S.P., Ignatius, A., Dürselen, L. & Seitz, A.M. (2021) Influence of menisci on tibiofemoral contact mechanics in human knees: a systematic review. *Frontiers in Bioengineering and Biotechnology*, 9, 765596. Available from: <https://doi.org/10.3389/fbioe.2021.765596>
 44. Tabbaa, S.M., Pace, J.L., Frank, R.M., Grammens, J. & Verdonk, P. (2023) Meniscus size differs between patient and

- donor populations for meniscus allograft transplantation. *Arthroscopy, Sports Medicine, and Rehabilitation*, 5(3), e569–e576. Available from: <https://doi.org/10.1016/j.asmr.2023.02.009>
45. Tack, A., Ambellan, F. & Zachow, S. (2021) Towards novel osteoarthritis biomarkers: multi-criteria evaluation of 46,996 segmented knee MRI data from the Osteoarthritis Initiative. *PLoS One*, 16(10), e0258855. Available from: <https://doi.org/10.1371/journal.pone.0258855>
46. Thorlund, J.B., Hare, K.B. & Lohmander, L.S. (2014) Large increase in arthroscopic meniscus surgery in the middle-aged and older population in Denmark from 2000 to 2011. *Acta orthopaedica*, 85(3), 287–292. Available from: <https://doi.org/10.3109/17453674.2014.919558>
47. Vicente, A.M., Ballensiefen, W. & Jönsson, J.-I. (2020) How personalised medicine will transform healthcare by 2030: the ICPeMed vision. *Journal of Translational Medicine*, 18(1), 180. Available from: <https://doi.org/10.1186/s12967-020-02316-w>
48. Willinger, L., Lang, J.J., Berthold, D., Muench, L.N., Achtnich, A., Forkel, P. et al. (2020) Varus alignment aggravates tibiofemoral contact pressure rise after sequential medial meniscus resection. *Knee Surgery, Sports Traumatology, Arthroscopy*, 28(4), 1055–1063. Available from: <https://doi.org/10.1007/s00167-019-05654-5>
49. Zaslav, K.R., Farr, J., Alfred, R., Alley, R.M., Dyle, M., Gomoll, A.H. et al. (2022) Treatment of post-menisectomy

knee symptoms with medial meniscus replacement results in greater pain reduction and functional improvement than non-surgical care. *Knee Surgery, Sports Traumatology, Arthroscopy*, 30(4), 1325–1335. Available from: <https://doi.org/10.1007/s00167-021-06573-0>

SUPPORTING INFORMATION

Additional supporting information can be found online in the Supporting Information section at the end of this article.

How to cite this article: Grammens, J., Van Haver, A., Danckaers, F., Vuylsteke, K., Sijbers, J., Mahluf, L. et al. (2024) Three-dimensional bone morphology is a risk factor for medial postmeniscectomy syndrome: a retrospective cohort study. *Journal of Experimental Orthopaedics*, 11, e12090. <https://doi.org/10.1002/jeo2.12090>